International Journal of Mechanical, Industrial and Aerospace Sciences
ISSN: 2517-9950
Vol:11, No:8, 2017

# Free Vibration Analysis of Functionally Graded Pretwisted Plate in Thermal Environment Using Finite Element Method

S. Parida, S. C. Mohanty

***Abstract*—**The free vibration behavior of thick pretwisted cantilevered functionally graded material (FGM) plate subjected to the thermal environment is investigated numerically in the present paper. A mathematical model is developed in the framework of higher order shear deformation theory (HOST) with $C^0$ finite element formulation i.e. independent displacement and rotations. The material properties are assumed to be temperature dependent and vary continuously through the thickness based on the volume fraction exponent in simple power rule. The finite element model has been discretized into eight node quadratic serendipity elements with node wise seven degrees of freedom. The effect of plate geometry, temperature field, material composition, and the modal analysis on the vibrational characteristics is examined. Finally, the results are verified by comparing with those available in literature.

***Keywords*—**FGM, pretwisted plate, thermal environment, HOST, simple power law.

## I. Introduction

FGM is a new advanced composite in which the properties of the constituent material vary continuously in a predetermined direction along thickness in a smooth pattern. Generally, FGM plate is preferred over conventional composite plate material to overcome the mode of failure due to interlaminar debonding of the constituent lamina that lead to instability of the fiber-reinforced laminated composite structure. FGMs are generally made from a mixture of ceramic and metal. The ceramic material due to its low thermal conductivity provides high-temperature resistance, and the ductile metal due to the high-temperature gradient helps in preventing fracture caused by stresses. Hence, the gradation in the properties reduces both thermal and residual stresses. In first order shear deformation theory (FOST), shear correction factors (SCFs) are introduced to rectify the discrepancy between the actual shear force distribution and those computed from the kinematic relation. HOST undergoes a cubic variation of the displacement such that, a more accurate stress distribution can be yielded. Pretwisted plates are structural elements with considerable technical significance. Extensive practical use of pretwisted plate can be found in aerospace, turbomachinery and other applications like aerial propeller and turbofans.

Nabi and Ganesan [1] analyzed the vibrational characteristics of glass fiber reinforced pretwisted composite blade using cylindrical, triangular shell element. Kee and Kim [2] studied the vibration analysis of a pretwisted rotating composite blade considering the Reissner-Mindlin's assumptions to examine the effect of Coriolis acceleration and centrifugal force. Leissa and Kadi [3] studied the influence of curvature on the frequency of shallow shells. Leissa et al. [4] employed Ritz method along with displacement functions in terms of the algebraic polynomial for the doubly curved cantilevered shallow shell. Jari et al. [5] investigated the static, free vibration, thermo-mechanical buckling of FGM plate using isogeometric approach and HOST. Based on third order shear deformation theory (TOST), Li et al. [6] presented the static and free vibration analysis of laminated composite plate using non-uniform rational B-splines (NURBS). Further, Li et al. [7] calculated the natural frequency using the three-dimensional linear theory of elasticity. Leissa et al. [8] obtained the theoretical and experimental result for free vibration of twisted, cantilevered plate of rectangular planform. Using the Rayleigh-Ritz technique, Sinha and Turner [9] investigated the free vibration behavior of the plate and derived the governing equation for the rotating pretwisted cantilever plate considering the Kirchhoff-von Karman's plate theory. A node based strain smoothening finite element is used for analyzing the static, free vibrational, thermal/mechanical buckling problems by Xuan et al. [10]. Reddy [11] derived the theoretical formulation for FGM plate that includes thermomechanical coupling and geometric nonlinearity using TOST. Reddy and Phan [12] adopted a refined shear deformation theory to present the exact solution for vibration and stability of the simply supported isotropic, orthotropic and laminated plate. Bazoune [13] considered the Southwell coefficient to present the in-plane and out of–plane frequencies to study the relation between rotating and non-rotating structures. Chandrashekhara [14] studied the free vibration behavior of laminated composite shells using isoparametric doubly curved quadrilateral shear element based on FOST. Zhu [15] studied the vibration analysis of rotating pretwisted Timoshenko beam and derived the kinetic energy, potential energy and the hybrid deformation variable using Rayleigh-Ritz method. The effect of rotating speed and pretwist angle on the frequency and damping ratio of the piezoelectric fiber reinforced composite material have been studied by Choi and Kim [16]. Hashemi [17] calculated the frequency for the rotating thick plate using Mindlin plate theory combined with assumptions regarding second order

S. Parida*, Research Scholar, and S.C. Mohanty, Associate Professor, are with the Department of Mechanical Engineering, NIT Rourkela, Rourkela: 769008 (*Corresponding author; e-mail: parida.smita10@gmail.com, scmohanty@nitrkl.ac.in).

strain displacement. Kane dynamic method has been employed for the non-linear strain analysis. Hu and Tsuiji [18] modeled a blade as a cylindrical panel with a twist and spanwise and chordwise curvature and derived governing equations for thin shell theory using the principle of virtual work using Rayleigh-Ritz method. Sreenivasmurthy and Ramamurti [19] investigated the effect of Coriolis acceleration term in kinetic energy expression on the first bending and first torsional frequency using finite element method for a flat rotating cantilever plate. Yang and Shen [20] analyzed the free and forced vibration FGM plate in uniform temperature using Galerkin approach. Kim [21] calculated frequency for the initially stressed plate employing the Rayleigh–Ritz procedure. Dokainish and Rawtani [22] employed the inertia force in addition to centrifugal force in order to calculate the natural frequency and mode shape of rotating cantilever plate. Huang and Shen [23] studied the nonlinear vibration characteristics of the FGM plate in the thermal environment.

There is hardly any literature available that deals with the pretwisted functionally graded thick plate in the framework of HOST in thermal environment using finite element method (FEM). The present work involves an eight-noded isoparametric element with nodal seven degrees of freedom using MATLAB. This paper presents an optimized displacement equation that satisfies the zero shear stress condition on either side of the plate. The material properties are graded along the plate thickness as per simple power law of distribution in terms of volume fraction. The material properties of the constituents are considered as temperature dependent. Comparison studies are provided to verify the accuracy and stability of the present method. The influences of parameters like volume fraction index, aspect ratio, thickness parameter, twist angle and the temperature on the frequency characteristics of the pretwisted FGM plate have been examined in details.

## II. Mathematical Formulation

Consider a pre-twisted plate with geometric dimensions of length $L$, width $B$ and total thickness $h$ clamped at its one side (left) with the opposite edge twisted at an angle $\phi$ as shown in Fig. 1.

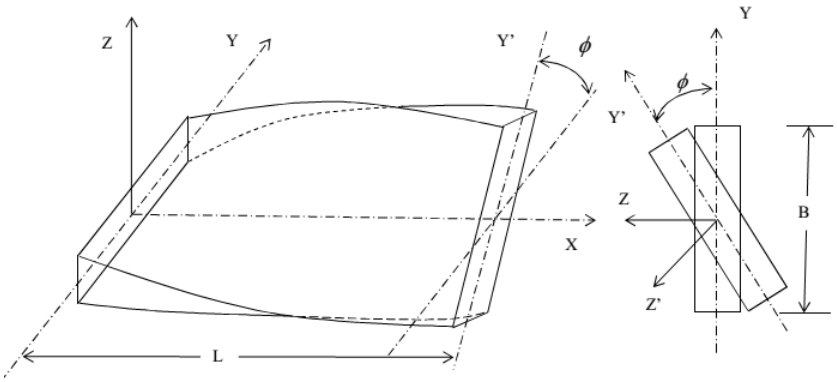


Fig. 1 A pretwisted plate

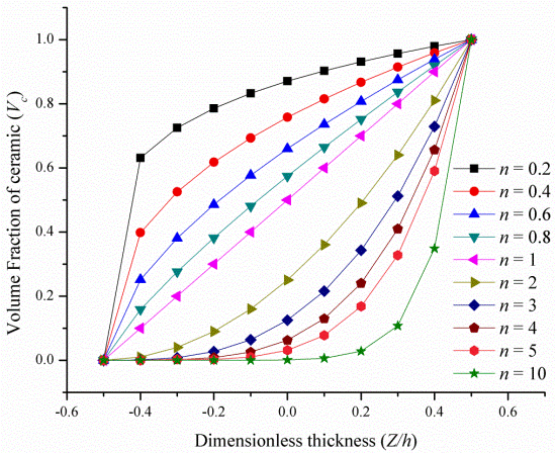


Fig. 2 Variation of volume fraction $V_c$ through the dimensionless thickness ($z/h$)

### A. Material Properties

The mechanical and thermal properties vary continuously along the interface between the two surfaces due to a gradual change in volume fraction of the constituent material obeying the simple power-law distribution of constituent volume fraction as shown in Fig. 2.

The material properties ($f$) are determined using the simple rule of mixture (Voigt model).

$$f(z) = f_c V_c + f_m V_m$$

where, $f_c, f_m$ and $V_c, V_m$ are the temperature-dependent material properties and volume fraction with subscript and $c$ and $m$ refers to ceramic and metal constituents. The volume fraction of the constituents (ceramic, metal) are obtained using the simple power law of distribution as

$$V_c + V_m = 1 \quad (1)$$

$$V_c = \left(\frac{z}{h}+\frac{1}{2}\right)^n,\ V_m = 1-\left(\frac{z}{h}+\frac{1}{2}\right)^n, \tag{2}$$

where, '$z$' is the thickness coordinate $(-h/2 \le z \le h/2)$ and '$n$' is the volume fraction index $(0 \le n \le \infty)$ responsible for generating an infinite number of varying composition.

The temperature-dependent material properties of the constituents like Young's modulus $E$, mass density $\rho$, thermal expansion coefficient $\alpha$, Poisson's ratio $\upsilon$ and the thermal conductivity $K_{eff}$ are expressed in terms of non-linear function of temperature, [25], as

$$f(z,T) = f_b(T) + \left[f_t(T) - f_b(T)\right]\left(\frac{z}{h}+\frac{1}{2}\right)^n \tag{3}$$

where, $f$ denotes an effective material property, $f_t$ and $f_b$ are properties of constituents at the top and the bottom of the plate. In this paper, metal is at the bottom $(z=-h/2)$ and ceramic is at the top $(z=+h/2)$.

$$f_m(T) \text{ and } f_c(T) = f_0\left(f_{-1}/T + 1 + f_1 T + f_2 T^2 + f_3 T^3\right) \tag{4}$$

where, $f_0, f_{-1}, f_1, f_2$ and $f_3$ are the coefficients of temperature $T$ (in K) responsible for characterizing the constituents.

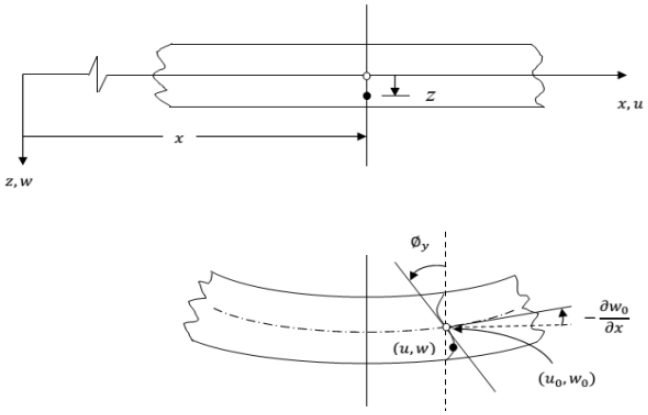


Fig. 3 FGM Plate before and after deformation

*B. Kinematics*

The FGM plate subjected to HOST presenting the parabolic distribution of transverse shear stress is shown in Fig. 3.

The displacement field for higher order theory, [26], is:

$$\begin{aligned}
\bar{u} &= u_0 + z\theta_y - \frac{4}{3h^2}\left(\theta_y + \frac{\partial w_0}{\partial x}\right)\\
\bar{v} &= v_0 - z\theta_x - \frac{4}{3h^2}\left(-\theta_x + \frac{\partial w_0}{\partial y}\right)\\
\bar{w} &= w_0
\end{aligned} \tag{5}$$

where, $\bar{u}$, $\bar{v}$ and $\bar{w}$ are the displacements of any point along the $(x, y, z)$ coordinates. $u_0, v_0, w_0$ and $\theta_x, \theta_y$ are the in-plane displacements and the rotations of transverse normal about the $x$ and $y$ axes, respectively. Due to the parabolic distribution of transverse shear stress, it represents a traction-free theory without any need of SCF, unlike FOST.

To convert the displacement equation into simple $C^0$ continuity, two new variables $\beta_x$ and $\beta_y$ are introduced by

$$\begin{aligned}
\bar{u} &= u_0 + z\theta_y - c_1 z^3\left(\theta_y + \beta_x\right)\\
\bar{v} &= v_0 - z\theta_x - c_1 z^3\left(-\theta_x + \beta_y\right)\\
\bar{w} &= w_0
\end{aligned} \tag{6}$$

where, $c_1 = 4/3h^2$, $\beta_x = w_{0,x}$, $\beta_y = w_{0,y}$

*C. The Stress-Strain Relationship*

The constitutive relation of an FGM plate in thermal environment is presented as

$$\begin{Bmatrix}\sigma_{xx}\\ \sigma_{yy}\\ \tau_{xy}\\ \tau_{xz}\\ \tau_{yz}\end{Bmatrix} = \frac{E(z,T)}{1-\upsilon^2}\begin{bmatrix}1 & \upsilon & 0 & 0 & 0\\ \upsilon & 1 & 0 & 0 & 0\\ 0 & 0 & \frac{(1-\upsilon)}{2} & 0 & 0\\ 0 & 0 & 0 & \frac{(1-\upsilon)}{2} & 0\\ 0 & 0 & 0 & 0 & \frac{(1-\upsilon)}{2}\end{bmatrix}\left(\begin{Bmatrix}\varepsilon_{xx}\\ \varepsilon_{yy}\\ \gamma_{xy}\\ \gamma_{xz}\\ \gamma_{yz}\end{Bmatrix} - \begin{Bmatrix}1\\ 1\\ 0\\ 0\\ 0\end{Bmatrix}\alpha\Delta T\right) \tag{7}$$

The strains can be expressed as

$$\varepsilon_{xx}=\frac{\partial u}{\partial x}=\left(\frac{\partial u_0}{\partial x}+\frac{w}{R_x}\right)+z\frac{\partial \theta_y}{\partial x}-c_1z^3\left(\frac{\partial \theta_y}{\partial x}+\frac{\partial \beta_x}{\partial x}\right)$$
$$\varepsilon_{yy}=\frac{\partial v}{\partial y}=\left(\frac{\partial v_0}{\partial y}+\frac{w}{R_y}\right)-z\frac{\partial \theta_x}{\partial y}-c_1z^3\left(-\frac{\partial \theta_x}{\partial y}+\frac{\partial \beta_y}{\partial y}\right)$$
$$\gamma_{xy}=\frac{\partial u}{\partial y}+\frac{\partial v}{\partial x}=\left(\frac{\partial u_0}{\partial y}+\frac{\partial v_0}{\partial x}+\frac{2w}{R_{xy}}\right)+z\left\{\frac{\partial \theta_y}{\partial y}-\frac{\partial \theta_x}{\partial x}+C\left(\frac{\partial v}{\partial x}-\frac{\partial u}{\partial y}\right)\right\}+c_1z^3\left(-\frac{\partial \theta_y}{\partial y}-\frac{\partial \beta_x}{\partial y}+\frac{\partial \theta_x}{\partial x}-\frac{\partial \beta_y}{\partial x}\right) \quad (8)$$
$$\gamma_{xz}=\frac{\partial u}{\partial z}+\frac{\partial w}{\partial x}=\left(\theta_y+\frac{\partial w_0}{\partial x}-\frac{u}{R_x}-\frac{v}{R_{xy}}\right)-c_2z^2\left(\theta_y+\beta_x\right)$$
$$\gamma_{yz}=\frac{\partial v}{\partial z}+\frac{\partial w}{\partial y}=\left(-\theta_x+\frac{\partial w_0}{\partial y}-\frac{v}{R_y}-\frac{u}{R_{xy}}\right)-c_2z^2\left(-\theta_x+\beta_y\right)$$

where, $C=\frac{1}{2}\left(\frac{1}{R_y}-\frac{1}{R_x}\right)$ is the result of Sanders theory for the condition of zero strain meant for rigid body motion. Equation (8) can be expressed as

$$\begin{Bmatrix}\varepsilon_x\\ \varepsilon_y\\ \gamma_{xy}\end{Bmatrix}=\begin{Bmatrix}\varepsilon_x^0\\ \varepsilon_y^0\\ \gamma_{xy}^0\end{Bmatrix}+z\begin{Bmatrix}\kappa_x^0\\ \kappa_y^0\\ \kappa_{xy}^0\end{Bmatrix}+z^3\begin{Bmatrix}\kappa_x^2\\ \kappa_y^2\\ \kappa_{xy}^2\end{Bmatrix}$$
$$\begin{Bmatrix}\gamma_{xz}\\ \gamma_{yz}\end{Bmatrix}=\begin{Bmatrix}\gamma_{xz}^0\\ \gamma_{yz}^0\end{Bmatrix}+z^2\begin{Bmatrix}\kappa_{xz}^1\\ \kappa_{yz}^1\end{Bmatrix} \quad (9)$$

Considering the displacement components of the HOST the governing equations of motion for twisted FGM plate are obtained using Hamilton's principle as

$$\delta u_0:\frac{\partial N_x}{\partial x}+\frac{\partial N_{xy}}{\partial y}-\frac{1}{2}\left(\frac{1}{r_y}-\frac{1}{r_x}\right)\frac{\partial M_{xy}}{\partial y}-\frac{Q_x}{r_x}-\frac{Q_y}{r_{xy}}=I_0\ddot{u}_0$$
$$\delta v_0:\frac{\partial N_y}{\partial y}+\frac{\partial N_{xy}}{\partial x}+\frac{1}{2}\left(\frac{1}{r_y}-\frac{1}{r_x}\right)\frac{\partial M_{xy}}{\partial x}-\frac{Q_x}{r_{xy}}-\frac{Q_y}{r_y}=I_0\ddot{v}_0$$
$$\delta w_0:\frac{N_x}{r_x}+\frac{N_y}{r_y}+\frac{2N_{xy}}{r_{xy}}+\frac{\partial Q_x}{\partial x}+\frac{\partial Q_y}{\partial y}=I_0\ddot{w}_0$$
$$\delta\beta_x:-\frac{4}{3h^2}\left(\frac{\partial P_x}{\partial x}+\frac{\partial P_{xy}}{\partial y}\right)-\frac{4}{h^2}R_x=-\frac{4}{3h^2}\left[I_4-\left(\frac{4}{3h^2}\right)^2I_6\right]\ddot{\theta}_y+\left(\frac{4}{3h^2}\right)^2I_6\ddot{\beta}_x$$
$$\delta\beta_y:-\frac{4}{3h^2}\left(\frac{\partial P_y}{\partial y}+\frac{\partial P_{xy}}{\partial x}\right)-\frac{4}{h^2}R_y=-\frac{4}{3h^2}\left[I_4+\left(\frac{4}{3h^2}\right)^2I_6\right]\ddot{\theta}_x+\left(\frac{4}{3h^2}\right)^2I_6\ddot{\beta}_y$$
$$\delta\theta_x:\frac{4}{3h^2}\left(\frac{\partial P_y}{\partial y}+\frac{\partial P_{xy}}{\partial x}\right)-\left(\frac{\partial M_y}{\partial y}+\frac{\partial M_{xy}}{\partial x}\right)-Q_y+\frac{4}{h^2}R_y=$$
$$\left[I_2+\left(\frac{4}{3h^2}\right)^2I_6\right]\ddot{\theta}_x+\frac{4}{3h^2}\left[I_4-\frac{4}{3h^2}I_6\right]\ddot{\beta}_y$$
$$\delta\theta_y:\left(\frac{\partial M_x}{\partial x}+\frac{\partial M_{xy}}{\partial y}\right)-\frac{4}{3h^2}\left(\frac{\partial P_x}{\partial x}+\frac{\partial P_{xy}}{\partial y}\right)+Q_x-\frac{4}{h^2}R_x$$
$$=\left[I_2-2\left(\frac{4}{3h^2}\right)I_4+\left(\frac{4}{3h^2}\right)^2I_6\right]\ddot{\theta}_y-\frac{4}{3h^2}\left[I_4-\frac{4}{3h^2}I_6\right]\ddot{\beta}_x \quad (10)$$

where, $(N_x,N_y,N_{xy}),(Q_x,Q_y)$ and $(M_x,M_y,M_{xy})$ present the total inplane force, shear force and moment resultant and $(P_x,P_y,P_{xy})$ and $(R_x,R_y)$ presents the higher order stress resultant.

$$\begin{Bmatrix}N_x\\ N_y\\ N_{xy}\end{Bmatrix}=\int_{-h/2}^{h/2}\begin{Bmatrix}\sigma_x\\ \sigma_y\\ \tau_{xy}\end{Bmatrix}dz,\ \begin{Bmatrix}M_x\\ M_y\\ M_{xy}\end{Bmatrix}=\int_{-h/2}^{h/2}\begin{Bmatrix}\sigma_x\\ \sigma_y\\ \tau_{xy}\end{Bmatrix}zdz,\ \begin{Bmatrix}P_x\\ P_y\\ P_{xy}\end{Bmatrix}=\int_{-h/2}^{h/2}\begin{Bmatrix}\sigma_x\\ \sigma_y\\ \tau_{xy}\end{Bmatrix}z^3dz$$
$$\begin{Bmatrix}Q_x\\ Q_y\end{Bmatrix}=\int_{-h/2}^{h/2}\begin{Bmatrix}\tau_{xz}\\ \tau_{yz}\end{Bmatrix}dz,\ \begin{Bmatrix}R_x\\ R_y\end{Bmatrix}=\int_{-h/2}^{h/2}\begin{Bmatrix}\tau_{xz}\\ \tau_{yz}\end{Bmatrix}z^2dz \quad (11)$$

## III. Nonlinear Temperature Rise

The nonlinear temperature rise along plate thickness can be obtained by solving one-dimensional Fourier equation of heat conduction. The heat conduction equation through the thickness is given by

$$-\frac{d}{dz}\left(K(z)\frac{dT}{dz}\right)=0 \quad (12)$$

The temperature variation through the thickness of an FGM plate can be calculated by imposing the boundary condition of $T=T_m$ at $z=-h/2$ and $T=T_c$ at $z=h/2$.

Substituting (3) for thermal conductivity in (12), the solution to the above equation can be solved using polynomial series. Considering the first seven terms, the obtained solution becomes

$$T(z)=T_m+\frac{\Delta T}{\mathrm{P}}\left[\begin{array}{l}\left(\frac{z}{h}+\frac{1}{2}\right)-\frac{K_{cm}}{(n+1)K_m}\left(\frac{z}{h}+\frac{1}{2}\right)^{n+1}+\frac{K_{cm}{}^2}{(2n+1)K_m{}^2}\left(\frac{z}{h}+\frac{1}{2}\right)^{2n+1}\\ -\frac{K_{cm}{}^3}{(3n+1)K_m{}^3}\left(\frac{z}{h}+\frac{1}{2}\right)^{3n+1}+\frac{K_{cm}{}^4}{(4n+1)K_m{}^4}\left(\frac{z}{h}+\frac{1}{2}\right)^{4n+1}\\ -\frac{K_{cm}{}^5}{(5n+1)K_m{}^5}\left(\frac{z}{h}+\frac{1}{2}\right)^{5n+1}\end{array}\right] \quad (13)$$

where,

$$\mathrm{P}=1-\frac{K_{cm}}{(n+1)K_m}+\frac{K_{cm}{}^2}{(2n+1)K_m{}^2}-\frac{K_{cm}{}^3}{(3n+1)K_m{}^3}+\frac{K_{cm}{}^4}{(4n+1)K_m{}^4}-\frac{K_{cm}{}^5}{(5n+1)K_m{}^5} \quad (21)$$

and $K_{cm}=K_c-K_m$. The stress resultant defined in (11) is related to the strains by

$$\begin{Bmatrix}\{N\}\\ \{M\}\\ \{P\}\end{Bmatrix}=\begin{bmatrix}[A] & [B] & [E]\\ [B] & [C] & [F]\\ [E] & [F] & [H]\end{bmatrix}\begin{Bmatrix}\{\varepsilon^0\}\\ \{\kappa^0\}\\ \{\kappa^2\}\end{Bmatrix}-\begin{Bmatrix}\{N^T\}\\ \{M^T\}\\ \{P^T\}\end{Bmatrix} \quad (14)$$

where, $\{N^T\}$, $\{M^T\}$ and $\{P^T\}$ are the thermal force and moment resultants

$$\{N^T\} = \int_{-h/2}^{h/2} \{\beta\}\Delta T dz, \qquad \{M^T\} = \int_{-h/2}^{h/2} \{\beta\}\Delta T z dz, \qquad \{P^T\} = \int_{-h/2}^{h/2} \{\beta\}\Delta T z^3 dz \tag{15}$$

where,

$$\{\beta\} = [Q]\{\alpha\} = \begin{Bmatrix} (Q_{11} + Q_{12})\alpha \\ (Q_{12} + Q_{22})\alpha \\ 0 \end{Bmatrix} \tag{16}$$

and $A$, $B$, $C$, $E$, $F$, $H$ are the plate stiffness

$$(A, B, C, E, F, H) = \int_{-h/2}^{h/2} Q_{ij}(1, z, z^2, z^3, z^4, z^6)dz \quad (i, j = 1, 2, 6)$$

and $Q_{ij}$ is the transformed elastic constant.

## IV. Finite Element Method

For the present analysis, an eight noded isoparametric quadratic serendipity plate element with nodal seven degrees of freedom (DOFs) has been considered for the finite element modeling, as given in Fig. 4.

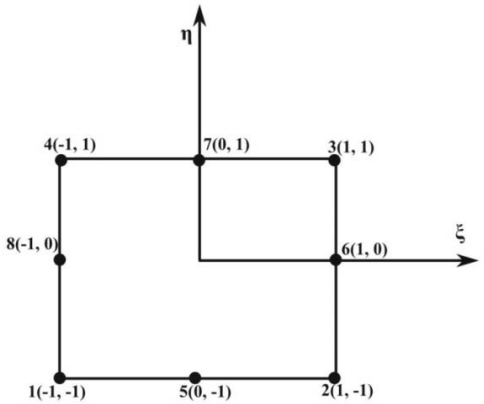


Fig. 4 An eight noded isoparametric serendipity element

The displacement vector in (6) can be presented as

$$\{\delta\} = \sum_{i=1}^{8} N_i^e(\xi, \eta)\ \{\delta_i\} \tag{17}$$

where, $\{\delta_i\} = \{u_{0i}, v_{0i}, w_{0i}, \beta_{xi}, \beta_{yi}, \theta_{xi}, \theta_{yi}\}$ is the node wise displacement field vector and $N_i$ is the interpolating vector dealt with $i^{th}$ node.

### A. Thermal Stiffness Matrix

The stress resulted due to thermal expansion in an FGM twisted plate

$$R_{th} = \int_A E(z,T)\alpha(z,T)\Delta T dA \tag{18}$$

where, $\alpha(z,T)$ is the co-efficient of thermal expansion of thermal expansion and $\Delta T$ is the steady state temperature change.

The work done by thermal load can be presented as

$$W_{th} = \frac{1}{2}\{\delta\}^T [K_{th}]\{\delta\} \tag{19}$$

The elemental thermal stiffness matrix

$$[K_{th}]_e = \int_{-1}^{1}\int_{-1}^{1} \left([N]^T R_{th}[N]\right) |J| d\xi d\eta \tag{20}$$

where, $[J]$ is the Jacobian matrix that transforms the global coordinate into local coordinate.

$$[J] = \begin{bmatrix} \sum_{i=1}^{8} \frac{\partial N_i}{\partial \xi} x_i & \sum_{i=1}^{8} \frac{\partial N_i}{\partial \xi} y_i \\ \sum_{i=1}^{8} \frac{\partial N_i}{\partial \eta} x_i & \sum_{i=1}^{8} \frac{\partial N_i}{\partial \eta} y_i \end{bmatrix}$$

### B. Elastic Stiffness Matrix

The strain energy of the twisted FGM plate can be expressed as

$$U = \frac{1}{2}\{\delta_i\}^T [K_e]\{\delta_i\} \tag{21}$$

The elemental stiffness matrixes is the collective sum of elemental bending and shear stiffness matrices and expressed as

$$[K]_e = [K_b]_e + [K_s]_e \tag{22}$$

$$[K_b]_e = \int_{-1}^{1}\int_{-1}^{1} \left([B_b]^T [D_b][B_b]\right)|J| d\xi d\eta \tag{23a}$$

$$[K_s]_e = \int_{-1}^{1}\int_{-1}^{1} \left([B_s]^T [D_s][B_s]\right)|J| d\xi d\eta \tag{23b}$$

where, $[B_b]$ and $[B_s]$ are bending and shear strain displacement matrices, respectively.

$$[B_b]_{1,1}=N_{i,x},\ [B_b]_{2,2}=N_{i,y},\ [B_b]_{3,1}=N_{i,y},\ [B_b]_{3,2}=N_{i,x},$$
$$[B_b]_{4,7}=N_{i,x},\ [B_b]_{5,6}=N_{i,y},\ [B_b]_{6,6}=N_{i,x},\ [B_b]_{6,7}=N_{i,y},$$
$$[B_b]_{7,4}=N_{i,x},\ [B_b]_{7,7}=N_{i,x},\ [B_b]_{8,5}=N_{i,y},\ [B_b]_{8,6}=N_{i,y},$$
$$[B_s]_{1,3}=N_{i,x},\ [B_s]_{1,7}=N_i,\ [B_s]_{2,3}=N_{i,y},\ [B_s]_{2,6}=N_i,$$
$$[B_s]_{3,4}=N_i,\ [B_s]_{3,4}=N_i,\ [B_s]_{4,5}=N_i,\ [B_s]_{4,6}=N_i$$
$$[B_b]_{9,4}=N_{i,y},\ [B_b]_{9,5}=N_{i,x},\ [B_b]_{9,6}=N_{i,x},\ [B_b]_{9,7}=N_{i,y}$$

*C. Mass Matrix*

The kinetic energy of the twisted FGM plate can be written as

$$T=\frac{1}{2}\{\delta_i\}^T[M]_e\{\delta_i\} \tag{24}$$

Elastic mass matrix,

$$[M]_e=\int_{-1}^{1}\int_{-1}^{1}[N]^T[I][N]|J|d\xi d\eta \tag{25}$$

where, $[I]$ and $[N]$ are the inertia and interpolating function matrix, respectively.

$$[I]_{1,1}=I_0,\quad [I]_{2,2}=I_0,\quad [I]_{3,3}=I_0,\quad [I]_{4,4}=c_1^2\times I_6,$$
$$[I]_{4,7}=-c_1\times(I_4-c_1I_6),[I]_{5,5}=c_1^2\times I_6,\quad [I]_{5,6}=c_1\times(I_4-c_1I_6),$$
$$[I]_{6,5}=c_1\times(I_4-c_1I_6),\quad [I]_{6,6}=I_2-2c_1(I_4-c_1I_6)+c_1^2I_6,$$
$$[I]_{7,4}=-c_1\times(I_4-c_1I_6),\quad [I]_{7,7}=I_2-2c_1(I_4-c_1I_6)+c_1^2I_6$$

where,

$$I_i=\int_{-h/2}^{h/2}\rho(z)z^i dz\quad (i=0,2,4,6),\quad c_1=\frac{4}{3h^2},\ c_2=3\times c_1$$

$$[N]_{1,1}=N_i,\ [N]_{1,1}=N_i,\ [N]_{1,1}=N_i,\ [N]_{1,1}=N_i$$
$$[N]_{1,1}=N_i,\ [N]_{1,1}=N_i,\ [N]_{1,1}=N_i$$

where, $N_i$ is the interpolating function at each node ($i$=1, 2, 3, 4, 5, 6, 7, 8)

## V. Results and Discussions

The numerical results of free vibration analysis of pretwisted FGM plate are calculated using the proposed finite element model of HOST using MATLAB. An eight noded quadratic serendipity finite element with nodal seven DOFs has been employed to discretize the plate. The validation and the accuracy test of the proposed method are done by comparing the obtained results with the published results available in the literature.

*A. Validation*

To validate the present finite element model, the calculated natural frequencies of a flat simply supported FGM plate are compared with those given by Bishop [24] as shown in Table I. The plate is made of Ti-6Al-4V/Aluminium Oxide and the geometric properties of FGM plate are $a$=$b$=0.4 m, $h$=0.005 m. Table II gives the comparison of non-dimensional frequency parameter ($\lambda$) of a cantilevered twisted plate for different angle of twists with published results of Nabi and Ganeshan [1] and Kee and Kim [2]. The notation $B$ denotes the spanwise bending frequency, $T$ the torsional frequency, *CB* the chordwise frequency, *EB* the edgewise bending frequency and $A$ the axial extension frequency. Table III shows the comparison of natural frequency parameter of $Si_3N_4$/SUS304 FGM plate with the results of Huang and Shen [23] at three different thermal loading conditions. It can be seen that the results agrees well with published results of Bishop [24], Nabi and Ganeshan [1], Kee and Kim [2] and Huang and Shen [23]. The mathematical formulations can be well trusted.

TABLE I
COMPARISON OF NATURAL FREQUENCY (HZ) FOR SIMPLY SUPPORTED TI-6AL-4V/ ALUMINIUM OXIDE FGM PLATE

| Mode | $n=0$ | | $n=2000$ | |
|---|---|---|---|---|
| | Present | Bishop [24] | Present | Bishop [24] |
| 1 | 144.9 | 145.04 | 271.28 | 271.23 |
| 2 | 362.4 | 362.61 | 677.93 | 678.06 |
| 3 | 362.4 | 362.61 | 678.00 | 678.06 |
| 4 | 580.3 | 580.18 | 1085.31 | 1084.9 |
| 5 | 726.9 | 725.22 | 1359.17 | 1356.1 |
| 6 | 727.0 | 725.22 | 1359.29 | 1356.1 |
| 7 | 947.3 | 942.79 | 1771.76 | 1763.0 |

TABLE II
COMPARISON OF FREQUENCY PARAMETER ($\lambda$) OF ISOTROPIC PRETWISTED PLATE

| Twist Angle ($\phi$) | Mode | Nabi and Ganeshan [1] | Kee and Kim [2] | Present |
|---|---|---|---|---|
| 0° | 1B | 3.46 | 3.49 | 3.46 |
| | 2B | 21.44 | 22.01 | 20.99 |
| | 1T | 8.53 | 8.51 | 8.35 |
| | 1CB | 27.05 | 27.33 | 26.70 |
| 30° | 1B | 3.41 | 3.42 | 3.402 |
| | 2B | 18.88 | 19.51 | 18.83 |
| | 1T | 16.88 | 14.43 | 15.96 |
| | 1CB | 27.98 | 27.41 | 27.38 |
| 45° | 1B | 3.36 | 3.35 | 3.32 |
| | 2B | 16.51 | 17.22 | 16.29 |
| | 1T | 22.31 | 20.45 | 24.35 |
| | 1CB | 30.40 | 28.76 | 29.93 |

TABLE III
NATURAL FREQUENCY PARAMETER FOR $Si_3N_4$/SUS304 SQUARE PLATE IN THERMAL ENVIRONMENT A=B=0.2M, H= 0.025M

| Temp(K) | Work | Volume fraction index (n) | | | | |
|---|---|---|---|---|---|---|
| | | Ceramic | n=0.5 | n=1 | n=2 | Metal |
| $T_c$=300 | Present | 12.587 | 9.094 | 7.656 | 6.780 | 5.445 |
| $T_m$=300 | Huang and Shen [23] | 12.495 | 8.675 | 7.555 | 6.777 | 5.405 |
| $T_c$=400, | Present | 12.387 | 8.615 | 7.510 | 6.642 | 5.311 |
| $T_m$=300 | Huang and Shen [23] | 12.397 | 8.615 | 7.474 | 6.693 | 5.311 |
| $T_c$=600, | Present | 11.971 | 8.272 | 7.186 | 6.327 | 4.989 |
| $T_m$=300 | Huang and Shen [23] | 11.984 | 8.657 | 7.544 | 6.669 | 4.971 |

*B. Parametric Study*

Non-dimensional frequency parameter

$$\bar{\lambda} = \omega \frac{a^2 \pi^2}{h} \sqrt{\frac{\rho_m (1-\upsilon^2)}{E_m}}$$

where, the material properties $\rho_m$, $E_m$ and $\upsilon_m$ refer to the values of metal at the reference temperature $T_0$=300K. Table IV shows the temperature-dependent properties of $Si_3N_4$/SUS304 FGM as given in Li et al. [7].

TABLE IV
TEMPERATURE DEPENDENT MATERIAL PROPERTIES OF CERAMIC AND METAL

| *Material* | $f_0$ | $f_{-1}$ | $f_1$ | $f_2$ | $f_3$ | *f(at 300K)* |
|---|---|---|---|---|---|---|
| | | | *$Si_3N_4$* | | | |
| *E* | 348.43 | 0 | -3.07e-13 | 2.160e$^{-16}$ | -8.946e-20 | 322.271 |
| *v* | 0.240 | 0 | 0 | 0 | 0 | 0.24 |
| *α* | 5.8723e-6 | 0 | 9.095e-6 | 0 | 0 | 7.4746e-6 |
| *ρ* | 2370 | 0 | 0 | 0 | 0 | 2370 |
| *K* | 9.19 | 0 | 0 | 0 | 0 | 9.19 |
| | | | *SUS304* | | | |
| *E* | 201.04 | 0 | 3.079e-13 | -6.534e-16 | 0 | 207.788 |
| *v* | 0.3262 | 0 | -2.002e-4 | 3.797e-7 | 0 | 0.3178 |
| *α* | 12.330e-6 | 0 | 8.086e-6 | 0 | 0 | 15.321e-6 |
| *ρ* | 8166 | 0 | 0 | 0 | 0 | 8166 |
| *K* | 12.04 | 0 | 0 | 0 | 0 | 12.04 |

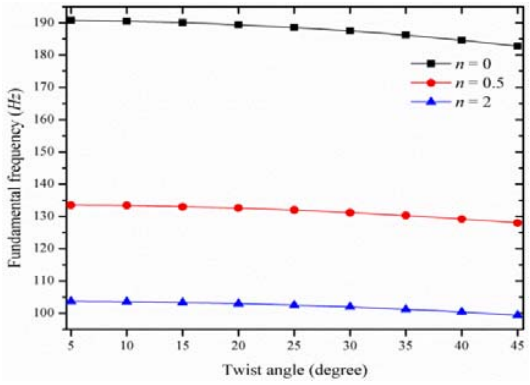


(a) Mode 1

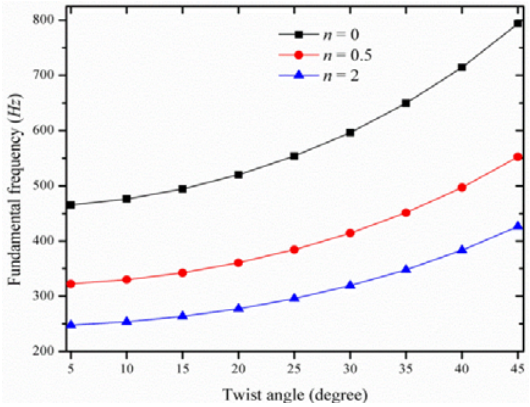


(b) Mode 2

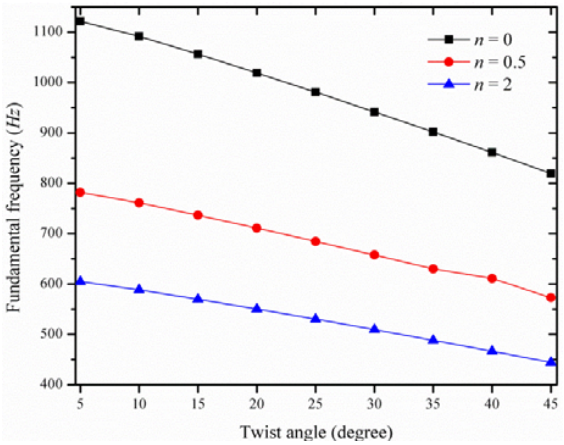


(c) Mode 3

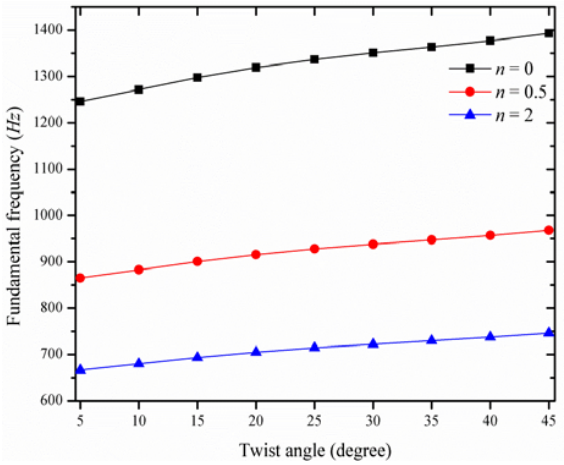


(d) Mode 4

Fig. 5 Variation of first four modes of frequency for different twist angles at thickness ratio ($a/h$=10) (a) mode1 (b) mode 2 (c) mode 3 (d) mode 4

Figs. 5 (a)-(d) show the effect of volume fraction index on first four natural frequencies for the thick cantilevered pretwisted FGM plate with the side thickness ratio ($a/h$=10) and unity aspect ratio with different twist angles. The frequency decreases with increase in twist angle and volume fraction index. The first mode represents the first bending mode (1B), the second mode represents the torsion mode (1T); the third mode represents the edgewise bending mode (1EB), and the fourth mode represents the second bending mode (2B). The spanwise bending (1$^{st}$ mode) frequency decreases with increase in twist angle. The decrease may be due to shear deformation and rotary inertia. The torsional mode increases with increases in pretwist angle, and this may be due to stretching of axially oriented elements near the parallel edges. It can be clearly noted that the increase in pretwist angle has a softening effect on first and third eigenvalue and a stiffening effect on second and fourth. The frequency decreases with increase in volume fraction index. This is because, with an increase in volume fraction index, the ceramic component

decreases thereby reduces the stiffness.

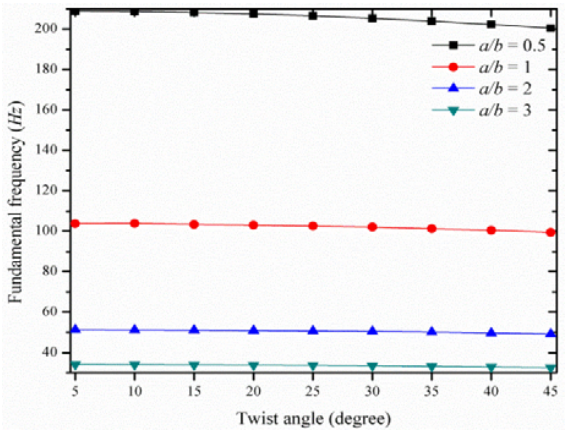


(a) Mode 1

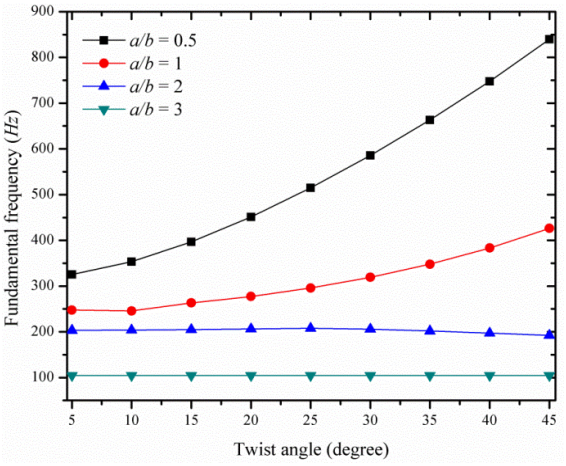


(b) Mode 2

Fig. 6 Variation of first two modes of frequency for different twist angles with side-thickness ratio ($a/h$=10) (a) mode 1 (b) mode 2

Figs. 6 (a) and (b) show the influence of aspect ratio on first two natural frequencies (Hz) of square $Si_3N_4$/SUS304 thick FGM plate with volume fraction index ($n$=2) of side-thickness ratio $a/h$=10 with varying twisting angle. The spanwise bending (1st mode) frequency decreases with increase in pretwist angle. The decrease may be due to shear deformation and rotary inertia. The second mode increases with increase in twisting angle that represents the torsional mode, and this may be due to stretching of axially oriented elements near the parallel edges. The effect of the pretwist angle seems to be significant with the plates of low aspect ratio than with higher aspect ratio.

Figs. 7 (a) and (b) represent first two natural frequencies for the cantilevered square pretwisted FGM plate ($n$=2) with varying thickness ratio ($a/h$=5, 10, 20, 30, 40, 50). In the first mode, the frequency decreases slightly with an increase in twist angle and also decreases with increase in thickness ratio. In the second mode, the frequency increases with increase in twist angle for low thickness ratio. The frequency of the FGM plate increases with increase in side thickness ratio and decreases with increase in twist angle. Fig. 8 shows the mode shape of functionally graded pretwisted plate with pretwist angle $\phi$=15˚ with varying aspect ratio and thickness ratio (a) $a/b$=1, $b/h$=20 (b) $a/b$ =1, $b/h$ =5 (c) $a/b$ =3, $b/h$ =20 (d) $a/b$ =3, $b/h$ =5

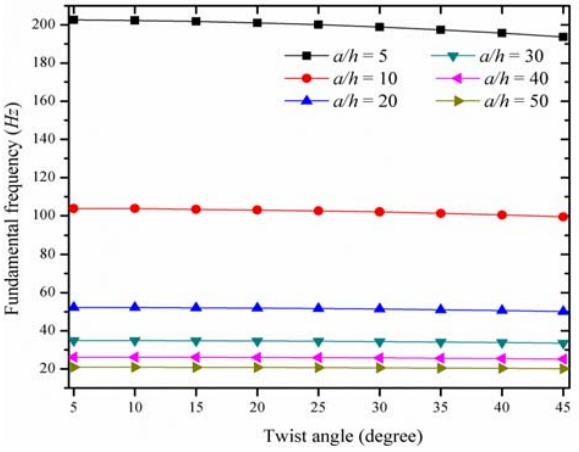


(a) Mode 1

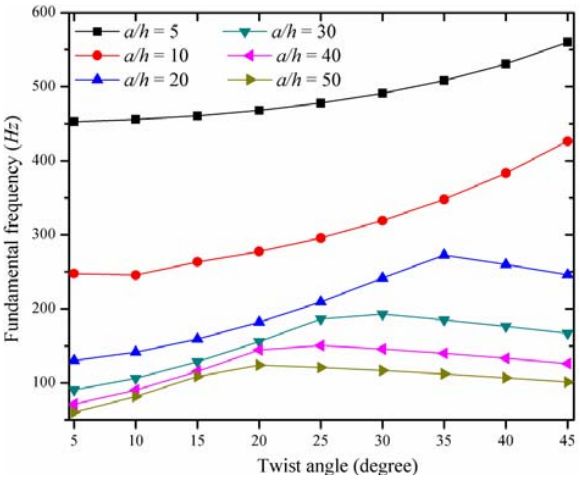


(b) Mode 2

Fig. 7 Variation of first two mode frequency with twist angle with $a/b$=1 (a) mode 1 (b) mode 2

In order to verify the present approach for vibration analysis in thermal environment, numerical results obtained for $Si_3N_4$/SUS304 square FGM plate in the thermal environment are compared with those of Huang and Shen [23] and is presented in Table IV. For further analysis in the thermal environment, the cantilevered pretwisted $Si_3N_4$/SUS304 FGM plate will be considered under different material properties ($n$), plate geometry (aspect ratio, thickness ratio) and temperature field.

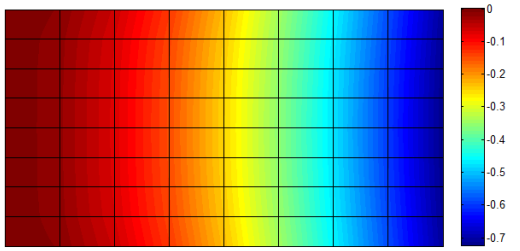


Mode 1 (1F)

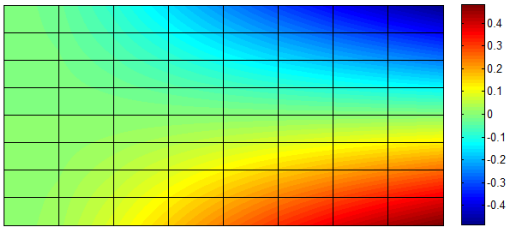


Mode2 (1T)

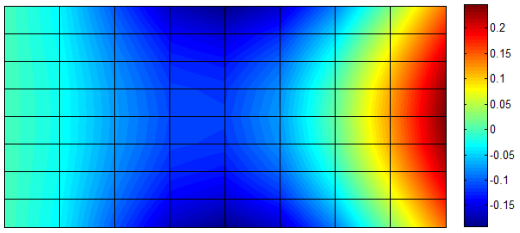


Mode 3 (2F)

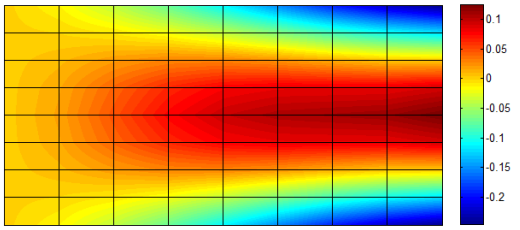


Mode 4 (1EB)

(a) First four modes for FGM plate with $a/b$=1, $h$=1/20, $\phi$ =15˚

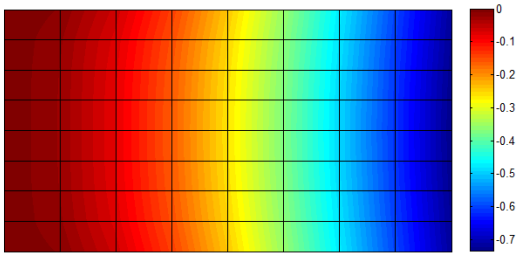


Mode 1 (1F)

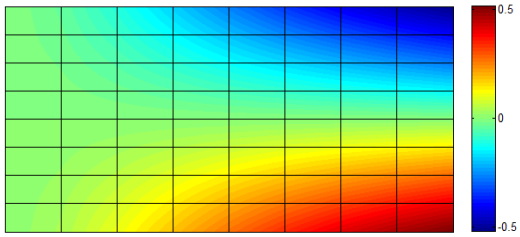


Mode2 (1T)

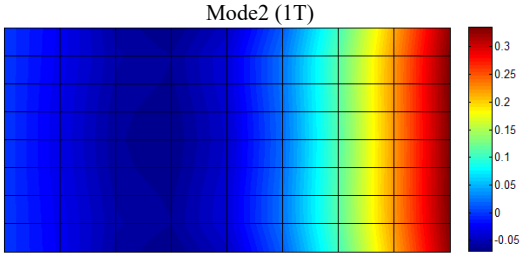


Mode 3 (2F)

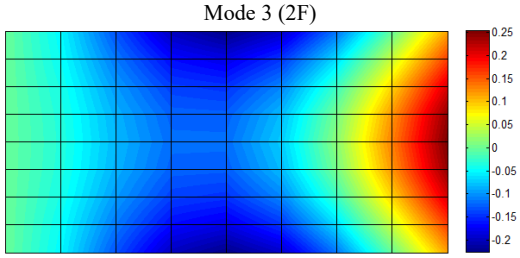


Mode 4 (2T)

(b) First four modes for FGM plate with $a/b$=1, $h$=1/5, $\phi$ =15˚

Fig. 8 Mode shapes of pretwisted FGM plate with pretwist angle ϕ =15˚ at different aspect ratio and thickness (a) $a$/b=1, $h$=1/20 (b) $a/b$=1, $h$=1/5

Non-dimensional frequency considered is defined as

$$\varpi = \omega \frac{a^2 \pi^2}{h} \sqrt{\frac{\rho_m}{E_m}}$$

where, the material properties $\rho_m$ and $E_m$ refer to the values of metal at the reference temperature $T_0$=300K.

Fig. 9 shows the frequency vs. temperature gradient for different volume fraction index ($n$). The frequency decreases with rise in temperature. This is because; with an increase in temperature the modulus of elasticity weakens and thereby reduces the stiffness. With the increase in volume fraction index, the ceramic component decreases and hence reduces the stiffness. Fig. 10 shows the frequency versus aspect ratio ($a/b$) for $Si_3N_4$/SUS304 twisted FGM plate ($\phi$ =15˚) at an elevated temperature of 100 K with the side thickness ratio $a/h$=10. Frequency decreases with increase in aspect ratio and volume fraction index.

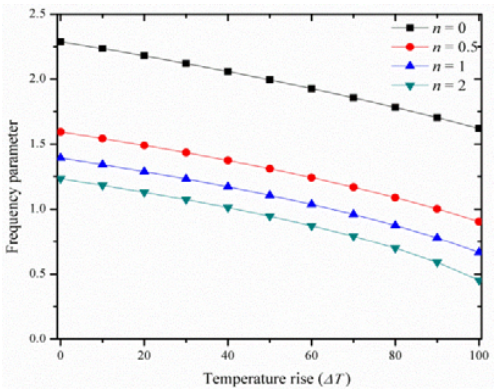


Fig. 9 The effect of temperature rise $\Delta T$ on frequency parameter ($\varpi$) with varying the volume fraction-index of a cantilevered pre-twisted $Si_3N_4$/SUS304

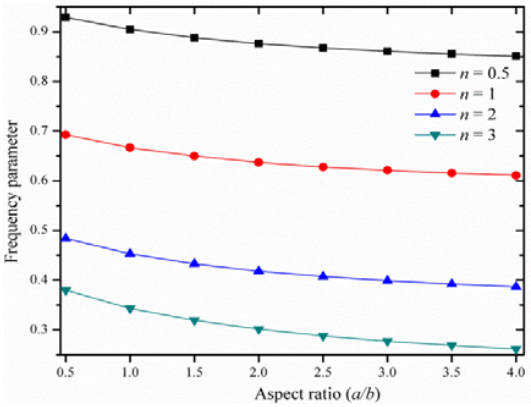


Fig. 10 The effect of volume fraction index on frequency parameter ($\varpi$) with varying aspect ratio $\phi$ =15$^0$, $\Delta T$=100 K

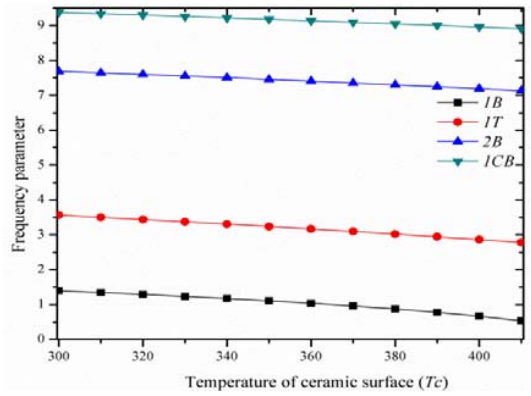


Fig. 11 First four modes of frequency for $Si_3N_4$/SUS304 FGM plate with varying temperature on ceramic surface

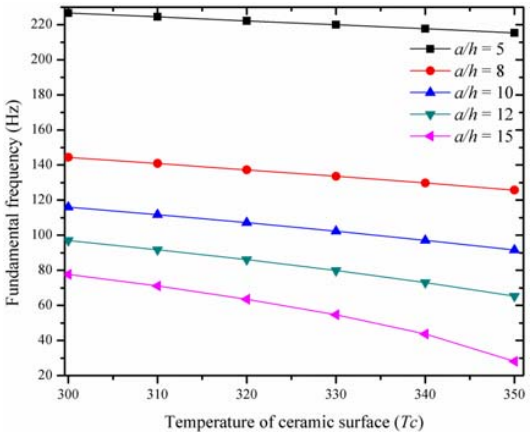


Fig. 12 The effect of side-thickness ratio on frequency parameter with varying temperature on ceramic surface of a twisted $Si_3N_4$/SUS304 FGM plate

Fig. 11 shows the effect of temperature and frequency for first four modes of frequency of pretwisted FGM plate ($\phi$=15˚) with side-width ratio $a/h$=10 and volume fraction index $n$=1. The frequency decreases with increase in temperature. This is because with an increase in temperature the young's modulus decreases. Fig. 12 shows the influence of side-thickness ratio on the fundamental frequency ($Hz$) for different temperature on ceramic surface for a pretwisted square $Si_3N_4$/SUS304 FGM plate ($\phi$ =15˚) with the aspect ratio $a/b$=1, $n$=1. The frequency decreases with increase in side thickness ratio. This is due to the effect of shear deformation and rotary inertia.

## VI. Conclusions

A higher order displacement field representing the inplane displacements and transverse displacement has been used to study the free vibration analysis of pretwisted cantilevered plate in the thermal environment using $C^0$ isoparametric formulation. The model is discretized into an eight-noded isoparametric element with seven degrees of freedom per node. The developed finite element model proves its accuracy by comparing the obtained results with the published results. The effect of various geometric parameters (twist angle, aspect ratio and side thickness ratio and temperature rise have been discussed in details.

## References

[1] S. M. Nabi and N. Ganesan, "Vibration and damping analysis of pre-twisted composite blades," *Comput. Struct.*, vol. 47, no. 2, pp. 275–280, 1993.

[2] Y. J. Kee and J. H. Kim, "Vibration characteristics of initially twisted rotating shell type composite blades," *Compos. Struct.*, vol. 64, no. 2, pp. 151–159, 2004.

[3] A. W. Leissa and A. S. Kadi, "Curvature effects on shallow shell vibrations," *J. Sound Vib.,* vol. 16, pp. 173–187, 1971.

[4] A. W. Leissa, J. K. Lee, and A. J. Wang, "Vibrations of cantilevered doubly-curved shallow shells," *J. Sound Vib.*, vol.3, pp. 311-328, 1983.

[5] H. Jari, H.R. Atri, S. Shojaee, "Nonlinear thermal analysis of functionally graded material plates using a NURBS based isogeometric approach," *Composite structures* vol. 119, pp. 333-345, 2015

[6] X. LI, J. Zhang, Y. Zheng, "Static and free vibration analysis of laminated composite plates using isogeometric approach based on the third order shear deformation theory," *Advances in mechanical engineering* 2014, pp. 1-16, 2014.

[7] Q. Li, V.P. Iu, K.P. Kou, "Three dimensional vibration analysis of functionally graded material plates in thermal environment," *J. Sound Vib.*, vol. 324, pp. 733-750, 2009.

[8] A. Leissa, J. Macbain, R. Kielb, "Vibration of twisted cantilevered plates-Summary of previous and current studies," *J. Sound Vib.*, vol. 96, pp. 159-173, 1984.

[9] S. K. Sinha and K. E. Turner, "Natural frequencies of a pretwisted blade in a centrifugal force field," *J. Sound Vib.*, vol. 330, no. 11, pp. 2655–2681, 2011.

[10] H. Nguyen-Xuan, L. V. Tran, C. H. Thai, and T. Nguyen-Thoi, "Analysis of functionally graded plates by an efficient finite element method with node-based strain smoothing," *Thin-Walled Struct.*, vol. 54, pp. 1–18, May 2012.

[11] J. N. Reddy, "Analysis of functionally graded plates," *Int. J. Numer. Methods Eng.*, vol. 684, no. June 1999, pp. 663–684, 2000.

[12] J. N. Reddy, N. D. Phan, "Stability and vibration of isotropic , orthotropic and laminated plates according to a higher-order shear deformation theory," *J. Sound Vib.*,, vol. 98, pp. 157–170, 1985.

[13] A. Bazoune, "Relationship between softening and stiffening effects in terms of Southwell coefficients," *J. Sound Vib.*, vol. 287, no. 4–5, pp. 1027–1030, 2005.

[14] K. Chandrashekhara, "Free vibrations of anisotropic laminated doubly curved shells," *Comput. Struct.*, vol. 33, no. 2, pp. 435–440, 1989.

[15] T. L. Zhu, "The vibrations of pre-twisted rotating Timoshenko beams by the Rayleigh-Ritz method," *Comput. Mech.*, vol. 47, no. 4, pp. 395–408, 2011

[16] S. C. Choi, J. S. Park, and J. H. Kim, "Vibration control of pre-twisted rotating composite thin-walled beams with piezoelectric fiber composites," *J. Sound Vib.*, vol. 300, no. 1–2, pp. 176–196, 2007.

[17] S. H. Hashemi, S. Farhadi, and S. Carra, "Free vibration analysis of rotating thick plates," *J. Sound Vib.*, vol. 323, no. 1–2, pp. 366–384, 2009.
[18] X. X. Hu, T. Tsuiji,"Free vibration analysis of curved and twisted cylindrical thin panels," *J. Sound Vib.*, vol. 219, pp. 63–88, 1999.
[19] S. Sreenivasamurthy and V. Ramamurti, "Coriolis effect on the vibration of flat rotating low aspect ratio cantilever plates," *J. Strain Anal. Eng. Des.*, vol. 16, no. 2, pp. 97–106, 2007.
[20] J. Yang and H.-S. Shen, "Vibration Characteristics and Transient Response of Shear-Deformable Functionally Graded Plates in Thermal Environments," *J. Sound Vib.*, vol. 255, no. 3, pp. 579–602, Aug. 2002.
[21] Y.-W. Kim, "Temperature dependent vibration analysis of functionally graded rectangular plates," *J. Sound Vib.*, vol. 284, no. 3–5, pp. 531–549, Jun. 2005.
[22] M. A. Dokainish, S. Rawtani, "Vibration analysis of rotating cantilever plates", *Int. J. Numer. Methods Eng.* vol. 3,pp. 233-248, 1971.
[23] X.L Huang, H.S Shen, ' Nonlinear vibration and dynamic response of functionally graded plates in thermal environments," *Int. J. solids and Struct.*, vol. 41, pp. 2403-2427, 2004.
[24] R.E.D. Bishop, "*The Mechanics of Vibration*", Cambridge University Press, New York, 1979.
[25] Touloukin YS. Thermophysical properties of high temperature solid materials, Macmillan, New York,1967
[26] Petyt M. Introduction to finite element vibration analysis , 2nd ed., Cambridge university press, 2010.